Real-Time Aerosol Measurements in Post-Combustion CO_2 Capture Using ELPI^{+TM} and Smooth and Sintered Collection Plates

Chiranjib Saha[1]

Southern Research,
Wilsonville, AL 35186;
National Carbon Capture Center (NCCC),
31800 Highway 25 North,
Wilsonville, AL 35186
e-mails: csaha@southernresearch.org;
x2csaha@southernco.com;
chiranjib.saha.ju@gmail.com

Justin H. Anthony

Southern Company Services, Inc.,
Wilsonville, AL 35186;
National Carbon Capture Center (NCCC),
31800 Highway 25 North,
Wilsonville, AL 35186
e-mail: jhanthon@southernco.com

The aerosols from CO_2-depleted flue gas at the National Carbon Capture Center (NCCC) Pilot Solvent Test Unit (PSTU) and Slipstream Solvent Test Unit (SSTU) were measured in real-time using a DEKATI Electric Low Pressure Impactor (ELPI^{+TM}). The coal-fired flue gas is provided by Alabama Power's Gaston Power Plant Unit 5. The utilization of ELPI^{+TM} for aerosol research in postcombustion CO_2 capture is very important due to its quick response time with size classification as low as 6 nm under transient conditions observed at the NCCC. Different process changes have been quantified at the PSTU and SSTU by multiple tests using the ELPI^{+TM}. The performance of smooth and sintered collection plates during dynamic process changes has been investigated. Between separate tests, upstream at unit 5, a new baghouse was installed. The aerosols measured at SSTU, before and after the baghouse installation, are compared. PSTU measurements demonstrated sample sensitivity to transient intercooler start-up conditions and dilution gas temperatures. During the tests, the typical concentration ranged from 10^6 to 10^7 cm^{-3}. The aerosol's counter median diameter (CMD) for the sintered plates are lower (47–60 nm) compared to the normal plates (89–130 nm). The optical images indicate that sintered plates soak up all of the collected aerosols. The aerosol number concentration showed a significant drop after the baghouse installation. These results are promising and will enable the development of process control strategies to mitigate solvent losses and reduce operation and maintenance expenses. [DOI: 10.1115/1.4038782]

Introduction and Background

Worldwide attention is increasingly focused on the control of CO_2 emissions from coal-based power generation [1]. At the same time, the demand for electric power is increasing in all parts of the world, and it is difficult to envision meeting the demand for power without the use of coal as a primary fuel [1,2]. To address the potential need for CO_2 emission control while still making use of coal and natural gas resources, it is becoming increasingly clear that the capture of CO_2 from existing power plants will be necessary [1,3].

To date, amine scrubbing appears to be the most promising technology for removing CO_2 from the flue gases of coal-fired power plants [4]. Pilot-plant tests and demonstrations have shown that CO_2 capture efficiencies in excess of 90% can be achieved in a properly designed scrubber system [1,5]. However, this process is associated with certain losses of amine due to thermal and oxidative degradation, vapor emission, and aerosol formation. Water wash after the absorber column has shown to be effective in reducing vapor emissions. However, emissions in the form of aerosols in the absorber section of pilot plants cannot be effectively removed by conventional emission counter-measures such as water wash [6].

Controlling aerosol-based solvent emissions requires detailed investigation [7]. Recent pilot plant studies have shown that amine aerosol emissions can be detrimental for commercial application of postcombustion solvent-based CO_2 capture technologies. The researchers at the National Carbon Capture Center (NCCC) are among the few in the world that started utilizing an Electrical Low Pressure Impactor (ELPI^{+TM}) for aerosol research in post-combustion CO_2 capture applications. The ELPI^{+TM} was ideal due to its quick response time with size classification as low as 6 nm under process conditions, which may be significantly transient like those observed. This paper describes the real-time aerosol measurement system and analytical techniques using the ELPI^{+TM} and presents results of the measurements. The results reported in this paper are for monoethanolamine solvent.

Process Descriptions and Test Methods

Several pilot scale amine-based postcombustion CO_2 capture test campaigns have been completed at the NCCC. It is important to understand the objective of this study for practical application of the results to scale up a postcombustion CO_2 capture system and hence described in this section. The pilot plant, ELPI^{+TM}, and sampling systems including the general operating procedure are also briefly described in this section.

Pilot Plants at the National Carbon Capture Center (NCCC). The NCCC is a state-of-the-art test center sponsored by the U.S. Department of Energy (DOE) and managed and operated by Southern Company. The NCCC is funded primarily by DOE along with a group of utility and industrial partners. Postcombustion CO_2 capture testing at the NCCC is conducted using a 0.5 MW_e slipstream of flue gas (35,000 lb/h max; 5000 lb/h nominal), downstream of the wet flue gas desulfurization system, from Alabama Power's Plant Gaston Unit 5 [8].

Figure 1 shows the process flow diagram of the Pilot Solvent Test Unit (PSTU). The measurement setup photos are shown in
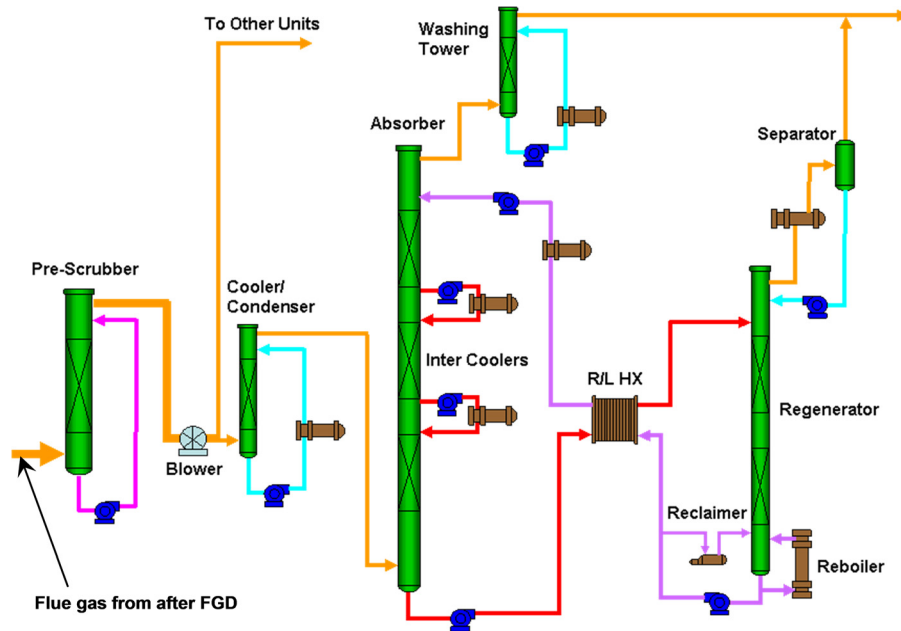

Fig. 1 Simplified process flow diagram of PSTU (FGD = flue gas desulphurization; R/L HX = rich/lean heat exchanger)
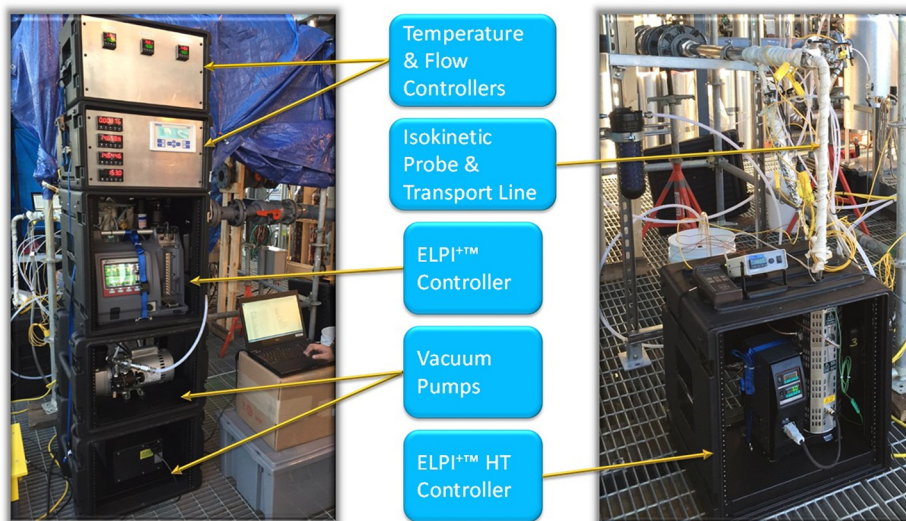

Fig. 2 ELPI^{+TM} measurement setup; photos taken during one of the test campaigns

Fig. 2. The details of the pilot plant subsystems can be found in Refs. [8] and [9]. Tests are also conducted at the Slipstream Solvent Unit (SSTU), which gets a nominal of 500 lb/h flue gas flow. The SSTU, fully integrated to the PSTU, is about one-tenth the size of the PSTU [9,10]. The aerosol size distributions and concentrations under different operating conditions are measured at the prescrubber inlet, absorber inlet, and wash tower outlet (WTO) locations using isokinetic probes and a DEKATI ELPI^{+TM}.

Objectives of This Study. The ultrafines and liquid mists, downstream of the combustion process, act as active sites for aerosols that have upper limits of 10 μm in diameter [11]. The aerosol formation process is described in Refs. [9] and [12]. Limitations of recently published studies (for e.g., not using the flue gas from commercial scale power plant, no operations under real-time process changes etc.) and the type of instruments used are mentioned in current literature [9,13–15]. In this study, the issues

identified earlier are addressed. In unit 5, a new baghouse was installed and began its operation in April 2016. The real-time aerosol characteristics before and after the baghouse installation are compared in this paper as the literature showed very few studies in this area related to the containment of the particulate emissions in the flue gas from coal combustion boiler [16]. The flue gas composition is mentioned in Table 1. The effect of ELPI^{+TM} impactor overloading has also been investigated under transient conditions to identify any significant variation in the aerosol characterization measurements when smooth and sintered aerosol collection substrates are used.
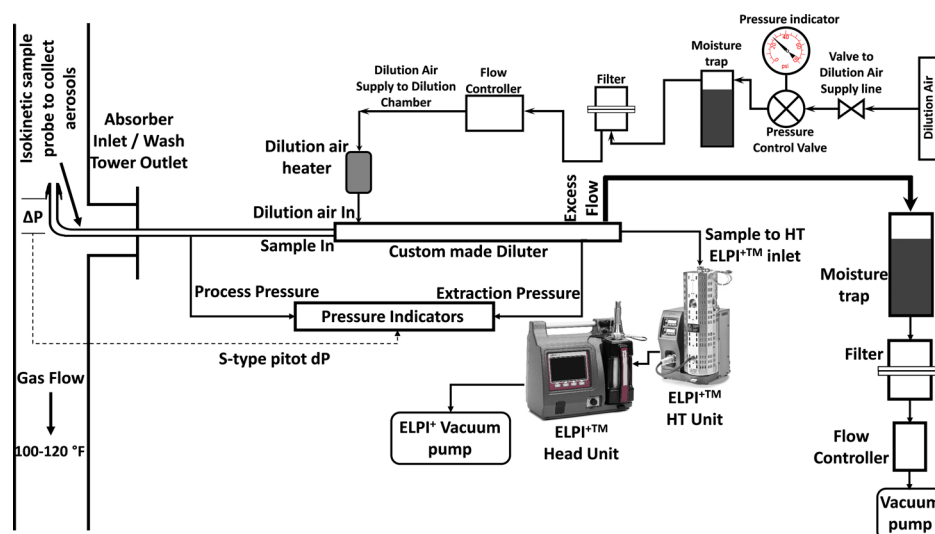
ELPI^{+TM} and Sampling Systems. The aerosol sampling device mainly consists of button hook nozzles connected with an extending sample probe to extract aerosols from the measurement locations, a dilution system to dilute the samples to avoid condensation on the collection substrates, the ELPI^{+TM} head unit, an

Table 1   Composition of the flue gas at different test locations

Test locations[a]	Avg. temp. (°F)	Avg. pressure (psi)	O_2 (vol %)	CO_2 (vol %)	H_2O (vol %)	SO_2 (ppm)	NO (ppm)	NO_2 (ppm)
Prescrubber inlet	129	−0.013	6.00	12.35	11.80	21.30	84.60	0.10
Absorber inlet	110	1.000	6.10	12.38	7.8	1.0	85.70	0.70
Wash tower outlet[b]	110	0.500	∼7.60	∼4.50	—	—	—	—

[a]Average values at the test locations are presented in the table.
[b]The gas composition at WTO really depends on capture rate, and many other conditions in the system. Therefore, a typical value for target 90% CO_2 removal is presented.

Fig. 3   Schematic of the isokinetic sample extraction system for ELPI^{+TM} measurements

elevated temperature chamber or high temperature ELPI^{+TM} unit (that contains all of the stages), and other accessories. The schematic of the measurement setup is shown in Fig. 3. The sample stream is expected to be saturated with moisture and thus heated air was used to dilute the sample for avoidance of condensation, which can lead to error in measurement due to electrical short circuiting, on the impactor plates. The importance of controlled dilution in aerosols or particulates measurement from power plant emissions has been relatively less addressed compared to the engine emissions research [17]. Probe internal heaters are used to heat the probe to maintain the gas temperature. The distance between sample nozzle extractions to dilution air point is less than 6 in.

Figure 4 shows the operating principle, the collection substrates, and stage assemblies. The operating principle of the ELPI^{+TM} is described in Refs. [9] and [18] and briefly mentioned here. The aerosols are first charged in a corona charger and then size classified from 0.006 to 10 μm in a low-pressure cascade impactor in real time. Electrometers, connected to each impactor stage, records an electrical current (proportional to the concentration of aerosols) produced by charged aerosols. Each impactor stage consists of a collection plate, a jet plate, and an insulator ring in the sequence from bottom to top as mentioned in the figure. The filter stage is the only one that has insulator on each side. The collection plates collect the aerosols after they pass through the nozzles in the jet plates. The insulators electrically isolate the plates from each other. In an ELPI^{+TM}, the sample containing different sized aerosols first passes through the jet plate nozzles. After the jet plate, the flow is directed toward the collection plate or substrate and makes a sharp turn to continue on to the next stage. Aerosols larger than a certain size are unable to complete the sharp turn and impact on the corresponding collection substrate. Aerosols smaller than a certain size remain in the flow. The operating principle of aerosol collection on different stages is

described in Fig. 5. In this way, the aerosols are size classified from 10 μm to 17 nm in the upper impactor stages and from 17 nm to 6 nm in the filter stage. The other specifications and operation limits are mentioned in Refs. [9] and [18]. The impactors, which have unique serial numbers, are calibrated by the manufacturer at certain pressure and temperatures that may differ from the pressure and temperatures at test conditions. Therefore, the D50% diameters are corrected. The DEKATI ELPI^{+TM} software also has the capability to correct the calibration, replay, and recalculate the data even after the real-time test and data collection is over. This is a great feature of the software to manage and analyze the data more effectively and in an efficient manner. Moreover, the temperature, flow, pumps, and all other related control systems are calibrated on a regular basis in order to achieve a high accuracy of the test results.

A high amount of collected particles can have a negative effect on the impactor performance, including the re-entrainment of previously collected particles. The gas flow pattern may also change affecting the cut diameter of each stage and in extreme cases the stage can even be clogged. In an ELPI^{+TM}, typically thin/aluminum foil smooth collection plate material is most widely used. While using these plates, particle, or aerosol impact, the collection plates with high velocity and may rebound from the "correct" stage into the following stage [18]. DEKATI recommends the use of a surface coating to prevent the bounce effect when using the smooth collection plates. For tests in this work where they were used, the authors have followed these recommendations and used DEKATI provided collection plate spray. However, the common problem of overloading or surface build-up for these kinds of substrates for this specific application was never investigated in postcombustion CO_2 capture aerosol research. It can be seen from the Figs. 4 and 5 that the measurements of aerosols are largely dependent on the characteristics, or real-time responses, of two physical components: the jet plates and collection plates in each
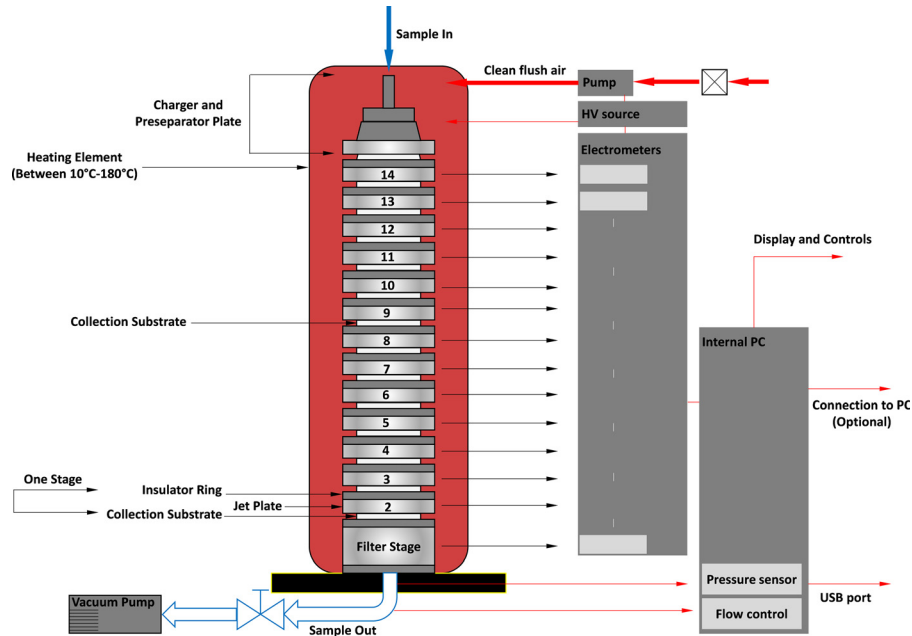
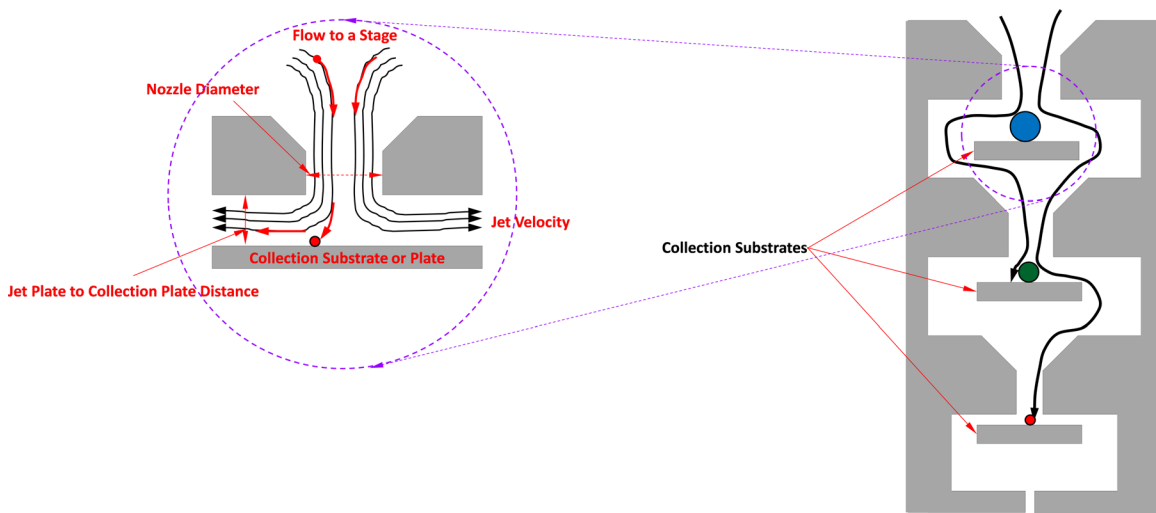**Fig. 4 Operating principle, collection substrates, and stage assemblies in high temperature ELPI^{+TM} unit**

Fig. 5 Operating principle of aerosol collection in different stages

impactor stage of an ELPI^{+TM}. However, the nozzle dimensions of a jet plate for an impactor stage are fixed so it is the difference of the collection plates' surface that may lead to nonidealities in aerosol measurements [18]. One such nonideal behavior of the ELPI^{+TM} is collection plate's surface build-up with aerosol, which is also commonly termed as "overloading." Therefore, several measurements are also conducted using the sintered plates and results are compared in this paper. Sintered plates consist of vacuum oil embedded in porous metal. The aerosols are collected on the plates and the oil seeps upward due to capillary forces. Thus, the impaction always occurs on a liquid surface effectively eliminating bouncing [18]. Figure 6 shows a smooth and a sintered collection plate before they were used in any test.

General Operating Procedure. The aerosol sampling setup and the ELPI^{+TM} are thoroughly cleaned before being operated. The sampler and the ELPI^{+TM} are turned on for 1–2 h prior to data collection allowing the equipment time for proper heat up and stabilization. During this period, the ELPI^{+TM} is in flush mode whereby the flow was reversed ensuring that no particles entered the device. The systems are thoroughly leaked, checked before every measurement, and the ELPI^{+TM} is carefully calibrated immediately before the test began in order to avoid any external effects on the measured currents in each stage.

Results and Discussions

Figure 7 represents the effect on total particle number concentration as measured real time by the EPLI^{+TM}. The X-axis represents the total test duration, primary Y-axis represents combined number concentration of all stages, and secondary Y-axis represents some of the absorber process parameters. The aerosol number concentration was generally in the range of 10^6 to 10^7 cm^{-3} at PSTU wash tower outlet before the installation of new baghouse. These results are in agreement with literature results [19]. As indicated by the absorber temperature profiles, both intercoolers were
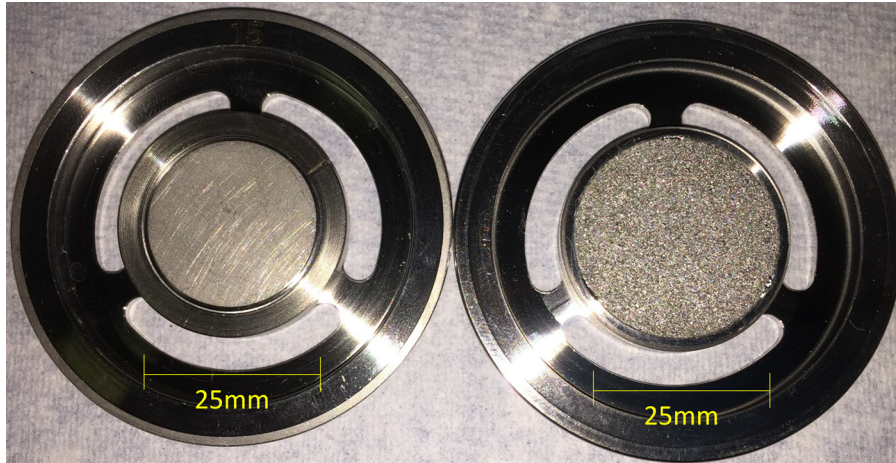
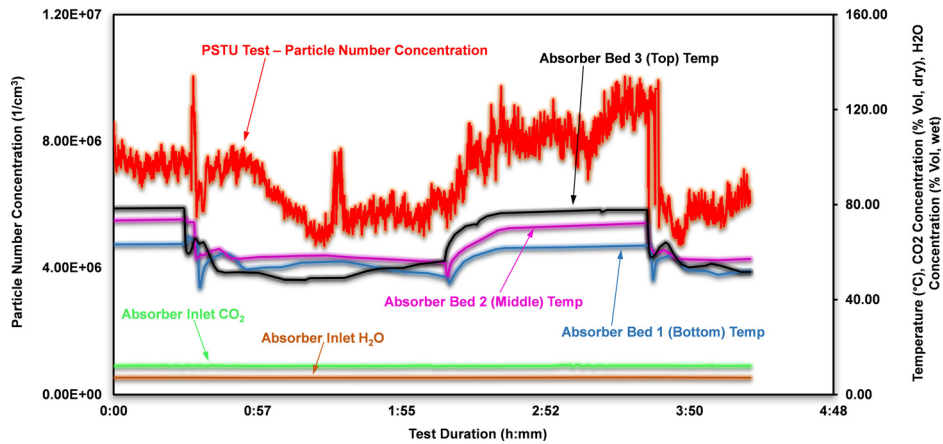**Fig. 6 (a) Normal smooth and (b) porous sintered collection plates**

Fig. 7 Real-time ELPI^{+TM} measurements of aerosol concentrations

turned on for two different periods (from 0:30 to 2:25 and 3:50 to 4:15 h of total test time). The intercoolers strongly influenced the particle concentrations, which generally decreased with decreasing absorber temperature.

The three-dimensional (3D) graphs in Fig. 8 display the particle size distribution as a function of time. X, Y, and Z axes show the aerodynamic particle size, time, and the concentration, respectively. A large number of aerosols with relatively higher size can be seen from the 3D graph when both the absorber intercoolers were off or not being operated. A plume of mist or aerosols was evident in the smallest size range immediately after the intercoolers were turned on as can be seen from the 3D plot. As time progressed, the total aerosol concentration eventually stabilized and decreased relative to the concentration before the start of the intercoolers (mentioned above in this section).

The real-time aerosol number concentrations at the dilution temperatures of 90 °C and 180 °C were measured. These results are compared in Fig. 9. A clear shift of higher number concentration toward lower sizes at the high dilution temperature can be seen. This size change is likely related to accelerated evaporation due to low relative humidity and elevated temperature of the aerosols. The larger aerosols may separate into much smaller particles and contribute to this higher number concentration at the lowest size fraction. Therefore, the process temperature should be just above the condensation point so that the aerosols are not vaporized or burst into smaller size fractions that are hard to capture.

Figure 10 shows the real-time ELPI^{+TM} measurements of aerosol number concentrations at the SSTU absorber inlet, wash tower outlets of the PSTU and SSTU and PSTU scrubber inlet. Very
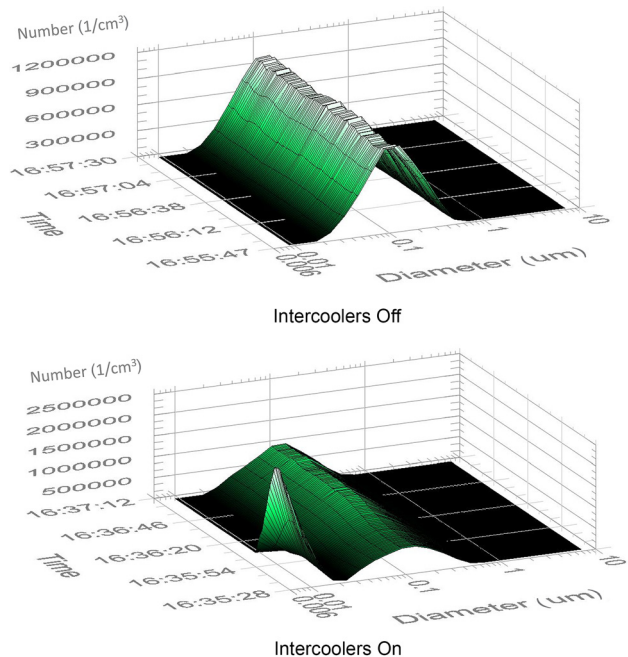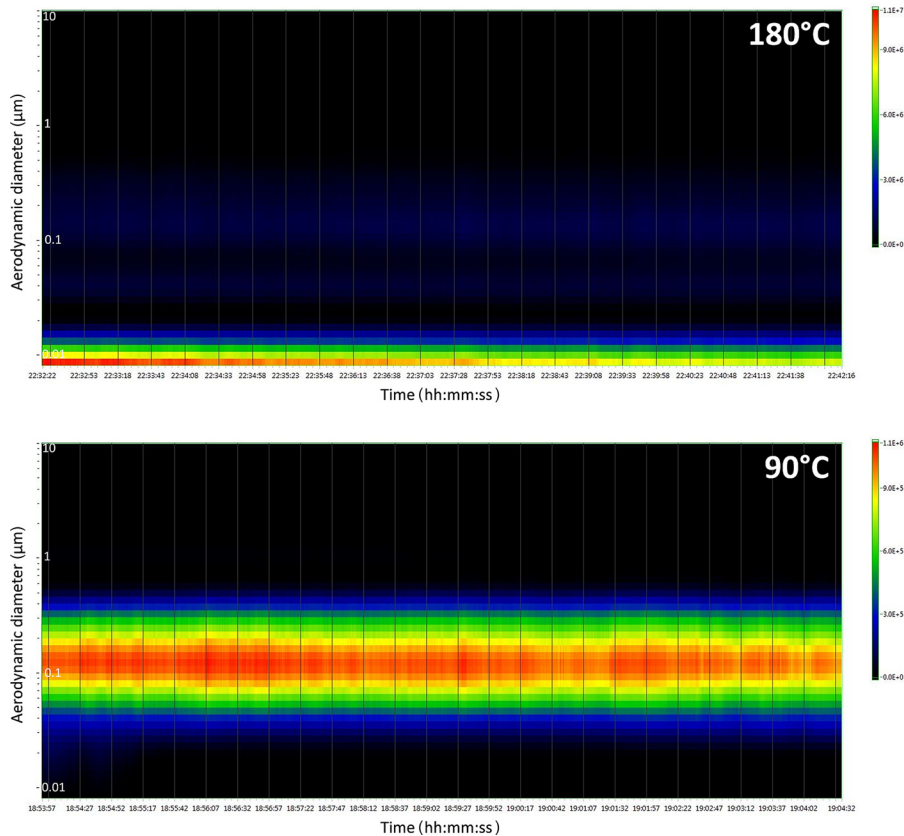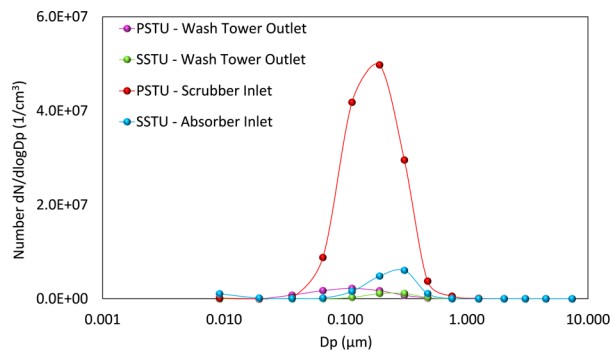

Intercoolers Off

Intercoolers On

Fig. 8 Effect of intercoolers on aerosol measured by ELPI^{+TM} in real time

Fig. 9   Effect of dilution heating temperature on real-time ELPI^{+TM} aerosol measurements
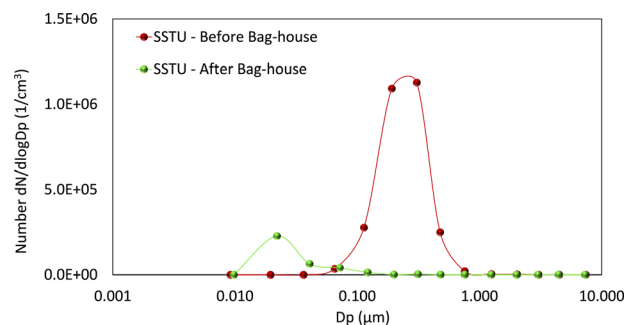
similar process and physical conditions are maintained during these sets of measurements [9]. As expected, the aerosol concentration is much lower at the SSTU wash tower outlet than at the SSTU absorber inlet. Similar aerosol concentrations can be observed at the SSTU and PSTU wash tower outlets. Figure 10 also shows the comparison of aerosol concentrations at the PSTU scrubber inlet and the wash tower outlet. It can be seen from the number concentration plots that the aerosol concentration is very high at PSTU scrubber inlet as compared to the wash tower outlet. The PSTU wash tower is a 23.5 in OD column with one bed of structured packing with a mist eliminator that is 1 ft in height. The packing type is Sulzer Mellapak plus M252.Y structured packing with 14 layers. The bed height is 9 ft 11 $\frac{1}{16}$ in. Total column height is 29 ft 8 in. The gas temperature at the outlet from wash tower is 110 °F. The circulation rate is 10,000 lb/h. This observation is expected, as the wash towers with the above specifications remove a substantial amount of aerosols. It can be clearly seen from Fig.

10 that the aerosol concentrations gradually decreases from scrubber inlet through absorber inlet to wash tower outlets. This behavior is expected and lowest concentrations can be seen at the wash tower outlets.

At unit 5 of Alabama Power's Plant Gaston, a new baghouse was installed and started its operation beginning April 2016. The real-time aerosol concentrations from the SSTU wash tower outlet before and after the baghouse installation are compared in Fig. 11. It can be seen that the aerosol numbers significantly dropped after the baghouse had been installed. The majority of the aerosols observed in the size range of 0.10–1.00 μm practically disappeared after the baghouse installation. However, aerosols in the size range of 0.01–0.10 μm are not completely captured at the wash tower outlet. This is expected because the smaller aerosols, although few in number, cannot be completely captured by a water wash. It is also observed that this significant drop in aerosol numbers is not strongly correlated to the plant's load indicating that aerosol counts are mostly irrespective of the plant's generation output. Therefore, it can be concluded that particulates from

Fig. 10   Comparison of real-time aerosol measurements at PSTU and SSTU

Fig. 11   Comparison of real-time aerosol measurements at SSTU before and after the baghouse installation
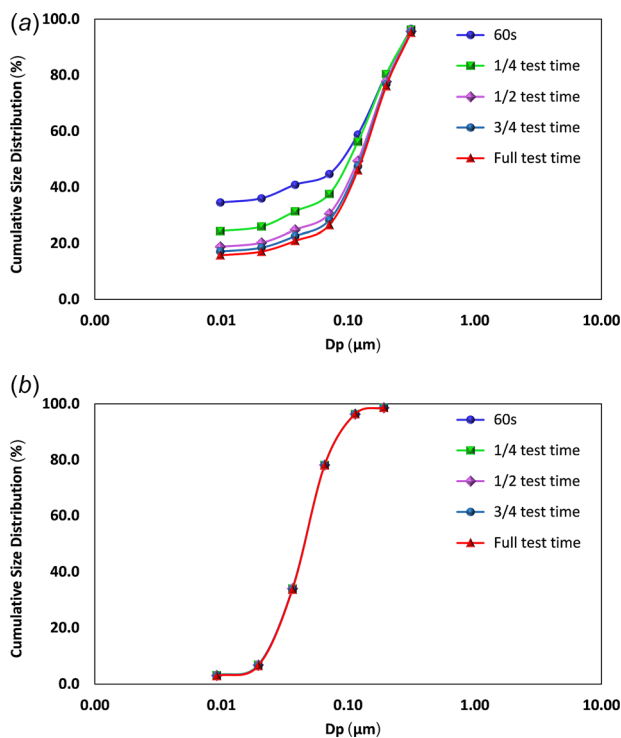
pyrolysis and ignition/burn-out of coal fines, intermediates, and coarse [20] are very well captured by the new bag house that helps to reduce the aerosol numbers significantly. Further investigation of these results is ongoing.

Aerosols are also measured in order to understand the performance of the smooth and sintered collection plates for ELPI^{+TM} operation. The cumulative size distributions are plotted in Fig. 12. Figures 12(a) and 12(b) show the cumulative size distributions for aerosols collected on smooth and sintered plates, respectively, at the wash tower outlet of the pilot plant. It should be noted that the cumulative size distributions are plotted over the sampling duration at specific intervals being at the start of the test (first 60 s), a quarter into the test time, initial half of the test time, three quarter into the test time and at the end of the test duration. The cumulative size distribution is a strong function of time with the ELPI^{+TM} under real-time measurement operation. Therefore, it is expected that the cumulative size distribution may change over time [21]. Thus, the results are plotted for different durations into the sampling test for visual representation of the potential effects of impactor overloading during transient conditions as mentioned above in the Objectives of This Study section. From Figs. 12(a) and 12(b), it can be seen that the aerosol cumulative size distribution changes with time during the tests when smooth collection plates are used, but the same is not true when sintered collection plates are used. This is a significant observation because if the size distribution is changing during a measurement, it is difficult to identify critical parameters necessary to design countermeasures of for aerosol mitigation. The results are further analyzed with the help of count median diameter (CMD) [22]. With regard to Fig. 12(a), CMD at the start of the measurement is 89 nm and increases to 103 nm, 121 nm, 126 nm, and 130 nm, respectively, with the progressive times mentioned earlier in this section. From Fig. 12(b), it can be seen that the cumulative size distribution for all the tests times overlap each other meaning the size distributions do not significantly vary with time. The average CMD for measurements during all the test times is 47 nm with a standard deviation of 0.07 nm. This parameter presents the greater
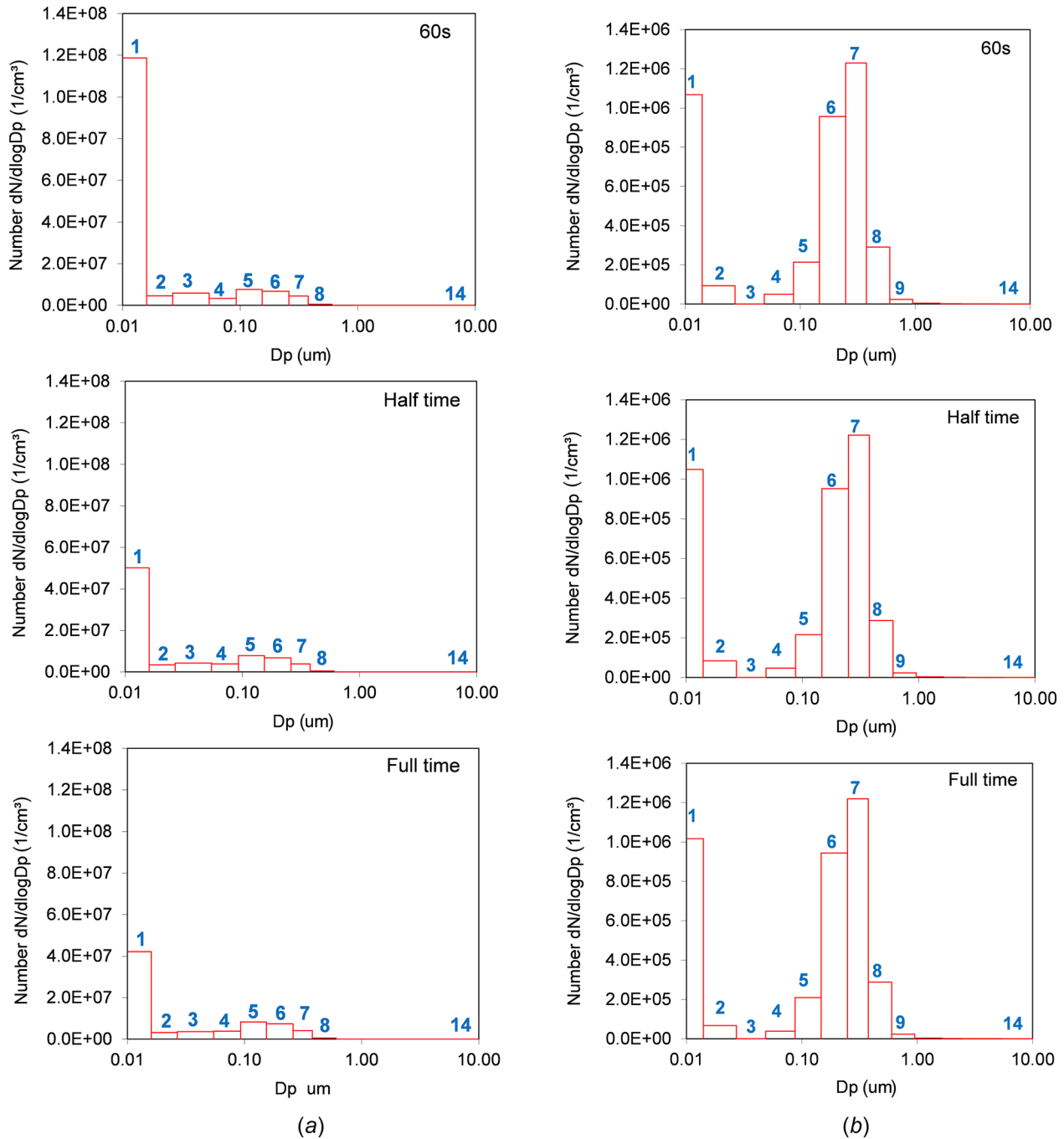
precision of aerosol measurements with sintered collection plates. Similar results are reported in literature [21]. Also, it has been reported that the total number concentration of particles is lower for lower CMD [23]. The change in CMD that is observed in Fig. 12(a) for different test times indicates that there may be some overloading of the smooth plates especially when the ELPI^{+TM} is used for real-time or dynamic measurements. The measurements have been carried out for a long enough time to make it believable that aerosols are sufficiently collected on the smooth plates. This may affect the gas flow path through the different stages (impactors, jet and collection plates) that in turn changes the CMD over the corresponding period of time. Although, when the ELPI^{+TM} is used with sintered plates, minimal changes in CMD are observed during real-time tests over prolonged periods indicating that the issue of impactor overloading is either minimized or eliminated. Similar observations are also reported in literature [21]. The results from additional prolonged measurements with images of the smooth and sintered collection plates after ELPI^{+TM} measurements are presented in the next paragraph.

In addition to the tests and results described above, two more tests are also completed in order to understand the performance of the smooth and sintered collection plates for continuous ELPI^{+TM} operation. The number concentrations for these tests during operation are presented in Figs. 13(a) and 13(b) for smooth and sintered plates, respectively. Similar to Fig. 12, the aerosol number concentrations are plotted at the start of the test (first 60 s), halfway into the test and at the end of the test for both cases investigated here. It should be noted that the aerosol number distribution significantly changed for the smooth plate case during the course of testing as can be seen from Fig. 13(a). The drop in concentration of 0.01 nm aerosols may be attributed to the drop in aerosol collection efficiency, which is a strong function of two important characteristics Stokes number (to characterize the behavior of aerosols suspended in sample flow) and Reynolds number (to predict the flow patterns of aerosols). Both the Stokes and Reynolds numbers are dependent on jet plate nozzle diameter, sample flow velocity, and stagnation properties [24,25]. During prolonged operation, the collection of aerosols on smooth plates is more as sintered plates soak up aerosols in their pores. The nozzle geometry and dimensions cannot be changed, so it may be the relatively higher accumulation of aerosols in case of smooth collection plates that alters the flow patterns by changing the Stokes and Reynolds numbers. In case of lower stages intended to record smaller size aerosol's concentration, the changes in Stokes and Reynolds number may be high that effect the collection efficiency in a high amount resulting in drop in aerosol concentration with progressive time. Further detailed investigation are ongoing and a focus area of future publications. However, the aerosol distribution in the case of sintered plates is mostly consistent throughout the test duration (Fig. 13(b)). These figures clearly indicate that after prolonged and continuous operation there may be relatively higher aerosol loading on the smooth plates compared to the sintered ones, which comparatively soak up the aerosols. However, the particulate deposition usually seen in diesel soot aerosol measurement applications using smooth collection plates is not observed here [26].

In order to further investigate this difference in results, the smooth and sintered collection plates are analyzed. Figures 14(a) and 14(b) show the optical images of smooth and sintered plates, respectively, after the continuous measurements have been completed. The plates for each case represent a typical stage collection plate and for simplicity all the stages that collected significant numbers of aerosols are not presented. It can be seen from Fig. 14(a) that aerosols accumulate on smooth plates during a test and remain after its completion. However, sintered plates soak up the aerosols in their pores as no pile up effect can be observed in Fig. 14(b). The central cores of the substrates are circled with a dotted line that clearly shows the collection effects for both cases. This is a critical observation when comparing to the unused substrates in Figs. 6(a) and 6(b). A presence of collected aerosols can be observed in the case of smooth plate in Fig. 14(a) compared to
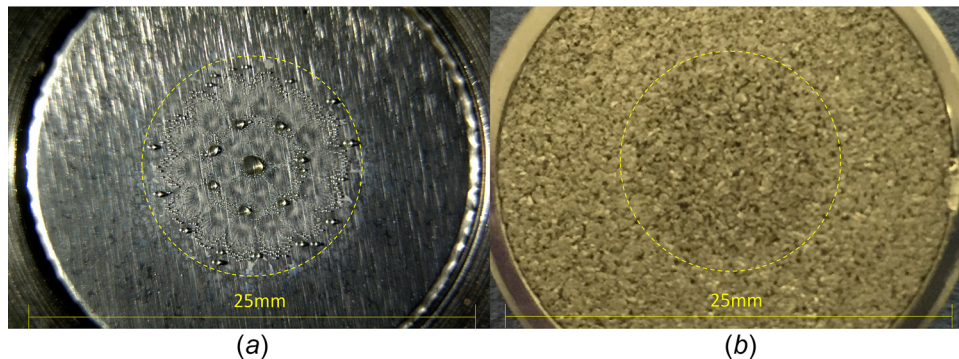

Fig. 12 Cumulative size distributions measured with (*a*) normal smooth and (*b*) porous sintered collection substrates at the WTO of pilot plant

Fig. 13 Changing aerosol number concentrations during continuous measurements with (*a*) normal and (*b*) sintered collection substrates for ELPI^{+TM}. Note: Numbers in Fig. 13 represent respective stages.

Fig. 6(*a*). However, for sintered plates in Fig. 14(*b*), the central portion is slightly darker due to liquid mist or aerosol soaking into them. Otherwise, this collection substrate after its use is very similar to the fresh sintered collection substrate as mentioned in Fig. 6(*b*). Therefore, these tests provide further evidence that there is a difference between aerosols loading when smooth and sintered collection plates are used for ELPI^{+TM} operation in postcombustion CO_2 capture pilot plants. Looking at the results from the literature related to diesel soot/aerosol measurements [26], it is believed that the aerosols do not rapidly overload the smooth collection plates for the test conditions investigated in this work. Moreover volatile components of diesel fuel play a significant role in aerosol concentration from engine emissions [27,28] as opposed to the aerosols from postcombustion CO_2 capture plants utilizing flue gas generated by coal combustion. However,

blending of coal-derived synthetic fuel and diesel although increases gas-phase emissions, but the particulates/aerosols emissions remain unchanged [29]. So, it is better to use porous sintered collection plates for aerosol characterization if necessary because using these plates will help the aerosols soaked up in their pores. So, there will be very minimum chance of collection substrates' overloading and hence minimizing the chance of artifacts in the results. However, if measurements are strictly targeted for gravimetric analysis, it is recommended to use normal smooth collection plates for better collection of mass and subsequent analysis. Therefore, the use of smooth plates is essential for prolonged collection of aerosols so that a substantial amount of aerosol is present for mass determination of based concentrations. The liquid and ultrafines within the aerosol droplets then can be subsequently analyzed for chemical composition and structural information.

Fig. 14 Optical images of (*a*) normal and (*b*) sintered collection substrates for a single stage after the use in continuous ELPI^{+TM} tests

Conclusions

Aerosols, carrying the amine, are measured in real-time using the ELPI^{+TM} and custom-made sampling systems at different sample locations of NCCC's pilot scale postcombustion CO_2 capture facilities utilizing the coal-fired flue gas from unit 5 of E.C Gaston power station. Aerosol concentrations were generally observed in the range of 10^6 to 10^7 cm^{-3} prior to baghouse installation but decreased with the use of intercoolers. The 3D plots clearly showed some smallest size range aerosols immediately after the intercoolers were put into service. The investigation of two different dilution scenarios revealed that the process temperature should be just above the condensation point so that the aerosols are not vaporized or burst into smaller size fractions that are hard to capture. The real-time aerosol concentrations progressively decreased when moved through the locations of prescrubber inlet, absorber inlet, and wash tower outlet of the pilot scale test unit. The installation of a new baghouse at Gaston Unit 5 decreased aerosol concentrations significantly and indications were that aerosol numbers are not dependent on the power station's load demand. The use of normal and sintered collection substrates clearly indicated that after prolonged and continuous operation, there is aerosol loading on the smooth collection plates compared to the sintered ones. However, it is believed that the aerosols do not rapidly overload the smooth collection plates for the test conditions investigated in this work. But it is better to use porous sintered collection plates for aerosol characterization if necessary except the measurements that are strictly targeted for gravimetric analysis. These promising results are intended to serve as the prerequisite for the analysis of different options to reduce aerosol emissions. Also, based on these results, further tests are planned under different parametric and long-term conditions and analysis of the results will be communicated through future publications.

Acknowledgment

U.S. Department of Energy (DOE) Required Disclaimer

Funding Data

Nomenclature

CMD	= count median diameter
DOE	= Department of Energy
ELPI	= electrical low pressure impactor
NCCC	= National Carbon Capture Center
O&M	= operation and maintenance
PSTU	= Pilot Solvent Test Unit
SSTU	= Slipstream Solvent Test Unit
WTO	= wash tower outlet

References

[1] Tola, V., Cau, G., Ferrara, F., and Pettinau, A., 2016, "CO_2 Emissions Reduction From Coal-Fired Power Generation: A Techno-Economic Comparison," ASME J. Energy Resour. Technol., **138**(6), p. 061602.
[2] Ruth, L. A., 2001, "Advanced Coal-Fired Power Plants," ASME J. Energy Resour. Technol., **123**(1), pp. 4–9.
[3] Cohen, S. M., Rochelle, G. T., and Webber, M. E., 2010, "Turning CO_2 Capture On and Off in Response to Electric Grid Demand: A Baseline Analysis of Emissions and Economics," ASME J. Energy Resour. Technol., **132**(2), p. 021003.
[4] Koytsoumpa, E.-I., Bergins, C., Buddenberg, T., Wu, S., Sigurbjörnsson, O., Tran, K. C., and Kakaras, E., 2016, "The Challenge of Energy Storage in Europe: Focus on Power to Fuel," ASME J. Energy Resour. Technol., **138**(4), p. 042002.
[5] Rokni, E., Chi, H. H., and Levendis, Y. A., 2017, "In-Furnace Sulfur Capture by Cofiring Coal With Alkali-Based Sorbents," ASME J. Energy Resour. Technol., **139**(4), p. 042204.
[6] Khakharia, P., 2015, "Aerosol-Based Emission, Solvent Degradation, and Corrosion in Post Combustion CO_2 Capture," Ph.D. thesis, Delft University of Technology, Delft, The Netherlands.
[7] Mertens, J., Anderlohr, C., Rogiers, P., Brachert, L., Khakharia, P., Goetheer, E., and Schaber, K., 2014, "A Wet Electrostatic Precipitator (WESP) as Countermeasure to Mist Formation in Amine Based Carbon Capture," Int. J. Greenhouse Gas Control, **31**, pp. 175–181.
[8] Southern Company Services, ed., 2012, "The U.S. Department of Energy Report—I," The National Carbon Capture Center at the Power System Development Facility, Wilsonville, AL.
[9] Saha, C., and Irvin, J. H., 2017, "Real-Time Aerosol Measurements in Pilot Scale Coal Fired Postcombustion CO_2 Capture," J. Aerosol Sci., **104**, pp. 43–57.
[10] Southern Company Services, ed., 2014, "The U.S. Department of Energy Final Report—I," The National Carbon Capture Center at the Power System Development Facility, Wilsonville, AL.

[11] Schaber, K., 1995, "Aerosol Formation in Absorption Processes," Chem. Eng. Sci., **50**(8), pp. 1347–1360.

[12] Brachert, L., Mertens, J., Khakharia, P., and Schaber, K., 2014, "The Challenge of Measuring Sulfuric Acid Aerosols: Number Concentration and Size Evaluation Using a Condensation Particle Counter (CPC) and an Electrical Low Pressure Impactor (ELPI$^+$)," J. Aerosol Sci., **67**, pp. 21–27.

[13] Chen, E., Fulk, S., Sache, D., Lin, Y., and Rochelle, G. T., 2014, "Pilot Plant Activities With Concentrated Piperazine," Energy Procedia, **63**, pp. 1376–1391.

[14] Mertens, J., Brachert, L., Desagher, D., Thielens, M. L., Khakharia, P., Goetheer, E., and Schaber, K., 2014, "ELPI$^+$ Measurements of Aerosol Growth in an Amine Absorption Column," Int. J. Greenhouse Gas Control, **23**, pp. 44–50.

[15] Khakharia, P., Brachert, L., Mertens, J., Huizinga, A., Schallert, B., Schaber, K., Vlugt, T. J. H., and Goetheer, E., 2013, "Investigation of Aerosol Based Emission of MEA Due to Sulphuric Acid Aerosol and Soot in a Post Combustion CO$_2$ Capture Process," Int. J. Greenhouse Gas Control, **19**, pp. 138–144.

[16] Thanisch, M. R., Rankin, D. M., Read, P. J., and Whaley, H., 1987, "The Performance of Fabric Filters in a Pilot Baghouse During Coal Water Fuel Combustion Trials," ASME J. Energy Resour. Technol., **109**(4), pp. 168–173.

[17] Fang, W., Kittelson, D. B., and Northrop, W. F., 2017, "Dilution Sensitivity of Particulate Matter Emissions From Reactivity-Controlled Compression Ignition Combustion," ASME J. Energy Resour. Technol., **139**(3), p. 032204.

[18] Dekati, 2015, "ELPI^{+TM} User Manual: Ver. 1.53," Dekati Ltd., Kangasala, Finland.

[19] Srivastava, R. K., Miller, C. A., Erickson, C., and Jambhekar, R., 2004, "Emissions of Sulfur Trioxide From Coal-Fired Power Plants," J. Air Waste Manage. Assoc., **54**, pp. 750–762.

[20] Taniguchi, M., Okazaki, H., Kobayashi, H., Azuhata, S., Miyadera, H., Muto, H., and Tsumura, T., 2001, "Pyrolysis and Ignition Characteristics of Pulverized Coal Particles," ASME J. Energy Resour. Technol., **123**(1), pp. 32–38.

[21] van Gulijk, C., Marijnissen, J. C. M., Makkee, M., and Moulijn, J. A., 2003, "Oil-Soaked Sintered Impactors for the ELPI in Diesel Particulate Measurements," J. Aerosol Sci., **34**(5), pp. 635–640.

[22] Hinds, W. C., 1999, *Aerosol Technology*, Wiley, New York.

[23] Maurya, R. K., and Agarwal, A. K., 2015, "Experimental Investigations of Particulate Size and Number Distribution in an Ethanol and Methanol Fueled HCCI Engine," ASME J. Energy Resour. Technol., **137**(1), p. 012201.

[24] Marjamaki, M., Ristimaki, J., Virtanen, A., Moisio, M., Luoma, R., and Keskinen, J., 2000, "Testing Porous Metal as a Collection Substrate in ELPI," J. Aerosol Sci., **31**(Suppl. 1), pp. S76–S77.

[25] Huang, C.-H., Tsai, C.-J., and Shih, T.-S., 2000, "Excess Particle Collection Efficiency by a Porous-Metal Substrate During Inertial Impaction Process," J. Aerosol Sci., **31**(Suppl. 1), pp. S130–S131.

[26] van Gulijk, C., Schouten, J. M., Marijnissen, J. C. M., Makkee, M., and Moulijn, J. A., 2001, "Restriction for the ELPI in Diesel Particulate Measurements," J. Aerosol Sci., **32**(9), pp. 1117–1130.

[27] Singh, A. P., and Agarwal, A. K., 2016, "Diesoline, Diesohol, and Diesosene Fuelled HCCI Engine Development," ASME J. Energy Resour. Technol., **138**(5), p. 052212.

[28] Zhang, C., Ge, Y., Tan, J., Li, L., Peng, Z., and Wang, X., 2017, "Emissions From Light-Duty Passenger Cars Fueled With Ternary Blend of Gasoline, Methanol, and Ethanol," ASME J. Energy Resour. Technol., **139**(6), p. 062202.

[29] Litzinger, T. A., and Buzza, T. G., 1990, "Performance and Emissions of a Diesel Engine Using a Coal-Derived Fuel," ASME J. Energy Resour. Technol., **112**(1), pp. 30–35.